Interreg
España - Portugal

Fondo Europeo de Desarrollo Regional
Fundo Europeu de Desenvolvimento Regional

Conocimiento sobre la determinación y caracterización de NPs de TiO_2 y Ag en la fracción bioaccesible y biodisponible en productos de acuicultura

- Acción 3 – Entregable 1 -

Metodologías operativas para el procedimiento de determinación y caracterización de NPs de TiO2 y Ag en la fracción de bioaccesibilidad in vitro

Procedimiento de bioaccesibilidad in vitro

El procedimiento de digestión in vitro se llevó a cabo por triplicado, pesando 0.5 g de pescado/molusco molido en matraces Erlemeyer de 100 mL. A continuación, se añadió un volumen de 20 mL de agua ultrapura y, tras 15 minutos, se ajustó el pH a 2,0 con una solución de ácido clorhídrico 0,1 M. A continuación, se añadieron 0.15 g de una solución gástrica recién preparada (pepsina 6,0 % (m/v) disuelta en ácido clorhídrico 6.0 M). Los frascos se taparon y se incubaron a 37 ºC con una agitación orbital - horizontal a 150 rpm durante 120 min. A continuación, los matraces se colocaron en un baño de agua helada para detener la digestión enzimática. Después de este tratamiento, el sobrenadante es la digestión gástrica in vitro.

El procedimiento continúa añadiendo al digesto gástrico 5.0 mL de la solución intestinal (pancreatina 4.0 %(m/v) y sales biliares 2.5 %(m/v) disueltas en bicarbonato de sodio 0.1 M). La digestión intestinal tuvo lugar en la incubadora a 37 ºC con una agitación orbital - horizontal a 150 rpm durante 120 min. La reacción enzimática se detuvo sumergiendo los frascos en un baño de agua helada. La fracción residual o no dializable (lodos restantes en los matraces) y la fracción bioaccesible (fase líquida) se sometieron a centrifugación (4 °C, 2500 rpm, 10 min) y la fase líquida se conservó para posteriores estudios de biodisponibilidad in vitro en células Caco-2.

Metodologías operativas de determinación y caracterización de NPs de TiO_2 y Ag en la fracción biodisponible mediante el procedimiento de digestión in vitro/procedimiento del modelo Caco-2

Procedimiento de digestión in vitro/modelo Caco-2

La fracción bioaccesible (7.5 mL) obtenida tras el procedimiento de digestión in vitro se calentó (baño de agua) a 100°C durante 5 minutos para inhibir la actividad de las enzimas gastrointestinales. Se añadió glucosa (concentración final 1 g L-1) y se ajustó la osmolaridad necesaria para la viabilidad celular (300 ± 25 mOsm kg-1) con NaCl (10 mM) en cada fracción bioaccesible (extracto).

Las células Caco-2 se mantuvieron en DMEM suplementado con 10% (v/v) de suero bovino fetal, 2mM de L-glutamina, 1% (v/v) de penicilina/estreptomicina, 1mM de piruvato sódico y 0.1mM de MEM, a 37°C bajo una atmósfera controlada con 95% de humedad relativa y un flujo de CO2 del 5%. El medio se cambió cada 2 o 3 días hasta alcanzar el 80% de confluencia. A continuación, las células se separaron con 0.5 g de tripsina y se resuspendieron en DMEM. Las células se sembraron (7.5 10^4 células cm^{-2}) en el inserto de membrana de poliéster en placas de 6 pocillos. El pocillo está dividido en dos compartimentos por el inserto; la cámara apical (superior) simula el lumen intestinal y la cámara basolateral (inferior) la cavidad serosa. Las células resuspendidas (1.5 mL) se añadieron a la cámara apical junto con 2 mL de DMEM. Para obtener una monocapa de células Caco-2, se colocaron en la cámara termostatizada a 37°C (95% de humedad relativa y un flujo de CO2 del 5%). Se midió la resistencia eléctrica transepitelial (TEER) para evaluar el progreso de la monocapa y se consideró adecuada una TEER de 250 mΩ cm^2.

El ensayo de transporte se realizó añadiendo 1.5 mL de fracción bioaccesible tratada a la cámara apical y 2 mL de HBSS a la cámara basolateral. Las monocapas se incubaron en las mismas condiciones de temperatura, humedad y CO_2 descritas anteriormente durante 60 minutos. Las soluciones apical y basolateral se retiraron y almacenaron hasta el análisis. Se añadió PBS (1.0 mL) a la cámara apical para lavar la monocapa celular. A continuación, se desprendieron las células con tripsina (4 min bajo temperatura controlada en la cámara termostatizada), y se retiraron de los pocillos.

Mediciones de NPs de TiO2 y Ag mediante sp-ICP-MS

Las fracciones apical, basal y celular se diluyeron 1:5 con glicerol al 1% (v/v), y las soluciones se sometieron a ultrasonidos (baño de agua con ultrasonidos, 37 kHz) durante 5 minutos antes de las mediciones de sp-ICP-MS (las condiciones de funcionamiento se resumen en la Tabla 1). Se midieron parámetros como el flujo de introducción de la muestra y la eficiencia de transporte antes de cada sección de medición. La eficiencia de transporte (TE%) se calculó analizando un material del NIST (Material de referencia: NPs de Au, 60 nm, 518 ng L^{-1}) en las mismas condiciones instrumentales que las muestras, pero controlando m/z 197 para el oro. Los valores válidos de TE% estaban dentro del rango de 1-5%. Se realizó una calibración acuosa de titanio y plata disueltos utilizando soluciones estándar de 0, 5, 10, 15 y 20 µg L^{-1}. El TE%, así como la calibración del Ti (Ag) disuelto, las concentraciones y distribuciones de tamaño de

las NPs de TiO_2 y Ag, y las concentraciones de Ti y Ag disueltas, se obtuvieron directamente del software de aplicación SyngistixTM Nano. Las condiciones de sp-ICP-MS se enumeran en la siguiente tabla.

Condiciones de Operación para sp-ICP-MS

Parametros Operación TiO_2 NPs	
Analito	Ti
Masa	48.9479 uma
Densidad	4.23 g cm^{-3}
Fracción Másica	59.9%
Eficiencia de Ionization	100%
Flujo Muestra	0.41 - 0.42 mL min^{-1}
Tiempo de Permanencia	100 µs
Tiempo Muestreo	100 s
Modo	Standard
Gas Celda A	0
RPa	0
RPq	0.5
Número escaneos	1
Número lecturas	25000
Replicas	3

Parámetros Operación Ag NPs	
Analito	Ag
Masa	106.905 uma
Densidad	10.49 g cm^{-3}
Fracción Másica	100 %

Eficiencia Ionización	100 %
Flujo Muestra	0.47 mL min^{-1}
Tiempo de Permanencia	50 µs
Tiempo Muestreo	100 s
Modo	Standard
Número de escáneres	1
Número de lecturas	100000

Interreg
España - Portugal

Fondo Europeo de Desarrollo Regional
Fundo Europeu de Desenvolvimento Regional

Conocimiento sobre el efecto del tratamiento (cocinado) del alimento sobre la biodisponibilidad de NPs de TiO_2 y Ag

- Acción 3 – Entregable 2/3 -

Conocimiento sobre el efecto del tratamiento (cocinado) del alimento sobre la biodisponibilidad de NPs de TiO_2 y Ag

Procedimiento de cocinado

Las muestras de almeja y dorada se sometieron a cocinado en plancha (sin aceite) y plancha a potencia media durante 5.0 min (cocinado por ambos lados). El procedimiento de cocción (sólo para dorada) consistió en cocer la muestra en 300 mL de agua ultrapura 90°C durante 10 min. Al finalizar la cocción, la muestra de dorada se escurrió y se dejo secar en estufa (40°C) durante 6.0 h.

Se determinó el porcentaje de agua de las muestras antes y después de someterlas al tratamiento culinario para así referir los contenidos de Ti y Ag y de nanopartículas de TiO_2 y Ag a peso seco (el cocinado implica pérdida de agua, y por tanto puede distorsionar los resultados al utilizar los resultados en peso húmedo de la muestra inicial y de la muestra cruda). El porcentaje de agua se calculó por diferencia de pesada tras someter las muestras a calor (horno a 90°C) hasta peso constante.

Procedimiento de bioaccesibilidad *in vitro* y de digestión *in vitro*/modelo Caco-2

Los procedimientos de digestión in vitro y de digestión *in vitro*/modelo Caco-2 se encuentran descritos en el Entregable 1 (Acción 3). Esta metodología se aplicó a muestras de almeja y dorada en crudo y tras los procedimientos culinarios de plancha (almeja y dorada) y cocción (dorada). En todos los casos se determinó el contenido total de Ti y Ag y las concentraciones de nanopartículas de TiO_2 y Ag en las muestras iniciales y tras los procesos de cocción mediante las metodologías ICP-MS y spICP-MS descritas en el Entregable 1 (Acción 3).

Bioaccesibilidad y transporte celular tras el cocinado

Los resultados (contenido total de Ti y Ag, y contenido de nanopartículas de TiO_2 y Ag) en las fracciones bioaccesibles y en las fracciones biodisponible (transporte celular) se muestran en la Tabla adjunta.

Especie		Bioacumulación				Biodisponibilidad					
		Extracción enzimática		Digestión ácida		Bioaccesiblilidad				Transporte celular	
		NPs g^{-1}		ng g^{-1}		NPs g^{-1}		ng g^{-1}		NPs g^{-1}	ng g^{-1}
		NPs	SD	Contenido total	SD	NPs	SD	Contenido total	SD	NPs	Contenido total
Almeja	**Ag**										
crudo		$7,23\ 10^{8}$	$1,68\ 10^{6}$	3,18	0,742	$1,28\ 10^{8}$	$9,56\ 10^{6}$	2,41	0,247	$1,91\ 10^{5}$	14,4
cocinado plancha		$4,55\ 10^{8}$	$5,75\ 10^{7}$	12,0	1,91	$9,60\ 10^{8}$	$1,11\ 10^{8}$	9,27	1,39	$4,55\ 10^{6}$	18,1
Almeja	**Ag**										
crudo		$3,28\ 10^{9}$	$8,28\ 10^{8}$	1,58	0,779	$9,12\ 10^{7}$	$8,51\ 10^{5}$	1,22	0,531	$2,85\ 10^{5}$	4,04
cocinado plancha		$4,74\ 10^{8}$	$5,11\ 10^{7}$	10,5	4,84	$1,78\ 10^{9}$	$1,36\ 10^{8}$	9,66	2,44	$6,32\ 10^{6}$	6,21
Almeja	**Ti**										
crudo		$5,14\ 10^{6}$	$1,21\ 10^{6}$	1,03	0,161	$9,31\ 10^{6}$	$7,71\ 10^{5}$	0,219	0,044	$2,18\ 10^{4}$	6,23
cocinado plancha		$4,97\ 10^{6}$	$3,01\ 10^{5}$	2,96	0,233	$6,29\ 10^{7}$	$4,60\ 10^{6}$	0,801	0,160	$3,31\ 10^{5}$	10,0
Almeja	**Ti**										
crudo		$3,06\ 10^{7}$	$9,10\ 10^{6}$	1,71	0,255	$5,13\ 10^{6}$	$4,77\ 10^{5}$	0,267	0,019	$5,85\ 10^{4}$	5,89
cocinado plancha		$1,11\ 10^{7}$	$9,01\ 10^{6}$	4,18	0,968	$8,15\ 10^{7}$	$4,06\ 10^{6}$	0,598	0,120	$8,33\ 10^{4}$	6,09
Dorada	**Ag**										
crudo		$4,25\ 10^{6}$	$2,04\ 10^{5}$	2,56	0,350	$1,18\ 10^{7}$	$1,75\ 10^{6}$	0,137	0,0663	$7,12\ 10^{5}$	0,113
cocinado plancha		$8,85\ 10^{5}$	$6,23\ 10^{4}$	3,17	0,244	$2,00\ 10^{7}$	$2,61\ 10^{6}$	1,05	0,0115	$1,21\ 10^{6}$	0,330
cocinado cocción		$8,01\ 10^{6}$	$3,59\ 10^{5}$	3,04	0,122	$3,77\ 10^{7}$	$5,06\ 10^{6}$	0,571	0,0931	$1,44\ 10^{6}$	0,391
Dorada	**Ti**										
crudo		$1,52\ 10^{6}$	$1,14\ 10^{5}$	0,117	0,003	$1,06\ 10^{7}$	$6,73\ 10^{5}$	0,094	0,019	$7,12\ 10^{4}$	5,74
cocinado plancha		$2,79\ 10^{6}$	$1,27\ 10^{6}$	0,862	0,506	$8,80\ 10^{7}$	$1,45\ 10^{6}$	0,234	0,047	$9,98\ 10^{4}$	6,52
cocinado cocción		$5,51\ 10^{6}$	$9,83\ 10^{5}$	0,170	0,035	$9,72\ 10^{7}$	$5,08\ 10^{6}$	0,078	0,016	$1,72\ 10^{5}$	6,88

En general, los procedimientos culinarios de cocción y plancha incrementan ligeramente los porcentajes de bioaccesibilidad y de permeabilidad celular de nanopartículas de TiO_2 y Ag.

Food Chemistry 360 (2021) 130002

Contents lists available at ScienceDirect

Food Chemistry

journal homepage: www.elsevier.com/locate/foodchem

Biopersistence rate of metallic nanoparticles in the gastro-intestinal human tract (stage 0 of the EFSA guidance for nanomaterials risk assessment)

María Vanesa Taboada-López, Gemma Vázquez-Expósito, Raquel Domínguez-González, Paloma Herbello-Hermelo, Pilar Bermejo-Barrera, Antonio Moreda-Piñeiro *

Trace Elements, Spectroscopy and Speciation Group (GETEE), Strategic Grouping in Materials (AEMAT), Department of Analytical Chemistry, Nutrition and Bromatology, Faculty of Chemistry, Universidade de Santiago de Compostela, Avenida das Ciencias, s/n., 15782 Santiago de Compostela, Spain

ARTICLE INFO

Keywords:
EFSA guidance
TiO_2 nanoparticles
Ag nanoparticles
In vitro gastrointestinal digestion
Biopersistence
Seafood

ABSTRACT

The European Food Safety Authority has published a guidance regarding risk assessment of nanomaterials in food and feed. Following these recommendations, an *in vitro* gastrointestinal digestion has been applied to study the biopersistence of TiO_2 and Ag NPs in standards, molluscs and surimi. TiO_2 NPs standards and TiO_2 NPs/ TiO_2 microparticles from E171 were not found to be degraded. Ag NPs proved to be more degradable than TiO_2 NPs, but the biopersistence rates were higher than 12%, which means that Ag NPs are also biopersistent. Findings for seafood are quite similar to those obtained for TiO_2 NPs and Ag NPs standards, although the calculation of the biopersistence rate proposed by the EFSA was not found to be straightforward for foodstuff (the use of the NPs concentration in the sample instead of the NPs concentration at initial time (sample mixed with the gastric solution before enzymatic hydrolysis) has been proposed.

1. Introduction

A nanomaterial (NM) is defined by the European Commission (EC) as a natural, incidental or manufactured material which contains at least 50% of particles with one or more dimensions between 1 and 100 nm (The European Commission, 2011). The novel mechanical, thermal, optical, and antimicrobial properties of NMs make them valuable ingredients in food science as additives for improving food appearance and lengthening shelf-life (Le-Guével, 2017). There are 119 listed NMs used in the food and beverage industry (Consumer Products Inventory, 2020), and inorganic nanoparticles (NPs), and more specifically metal and metal-oxide NPs, are widely used as food additives and as active ingredients in films for food packaging (Le-Guével, 2017). However, the impacts of engineered NMs on environmental and human health are unclear, and research for elucidating the potential risks is a current challenge (Holland & Zhong, 2018).

Titanium dioxide (TiO_2) as a bulk material is the authorised food additive E171 and it is used as a pigment since the high refractive index and brightness (Weir et al., 2012), and foods such as candies, sweets, chewing gums, cheese and cheese products, edible ices, crab sticks (surimi), dressings, and non-dairy creamers contain E171 (Geiss et al., 2020). Several studies on food-grade E171 have reported the presence of TiO_2 NPs in a number-based fraction ranging from 17 to 36% (Yang et al, 2014).

The antimicrobial activity exhibited by TiO_2 NPs and silver (Ag) NPs has led to their use as active ingredients in food packaging (Ogunsona et al, 2020; dos Santos et al., 2020; Mei & Wang, 2020; Sharma et al., 2020). TiO_2 NPs show a strong oxidizing power when illuminated with ultraviolet (UV) light (385 nm), which enhances the production of reactive oxygen species (ROS) and promotes the breakdown of bacteria membranes (Yemmireddy & Hung, 2015a; Venkatasubbu et al., 2016). Similarly, the antibacterial mechanism of Ag NPs is related to the formation of ROS (Akter et al., 2018), and there are some insights regarding Ag NPs transcellular transport and endocytosis after crossing the cytoplasmic membrane and oxidizing into Ag ions (Ag^+) (Murugan et al., 2015; Zheng et al., 2018). Nevertheless, the antibacterial activity of TiO_2 NPs has been demonstrated to depend on the food composition as well as turbidity and oxygen (Yemmireddy & Hung, 2015b).

There is great concern regarding the migration of NPs from packaging to food products or their direct use as additives in foodstuff. The interaction between NPs and food matrix can affect the physicochemical and morphological properties of NPs, as well as their biotransformation, gastrointestinal fate, and bioactivity. Food constituents, molecular interactions, and structural organization are important food properties

* Corresponding author.
E-mail address: antonio.moreda@usc.es (A. Moreda-Piñeiro).

https://doi.org/10.1016/j.foodchem.2021.130002
Received 7 December 2020; Received in revised form 6 April 2021; Accepted 30 April 2021
Available online 5 May 2021

that have a potential impact on NPs behaviour (McClements et al., 2017). Physicochemical properties of NPs can also be modified during food ingestion, digestion, and fermentation. The presence of enzymes, the ionic strength and pH changes are important factors that can modify the bioavailability of NPs by *in vitro* procedures (Laloux et al., 2017).

The European Food Safety Authority (EFSA) published a guidance in 2018 to evaluate the risks of the application of nanoscience and nanotechnologies in the food and feed chain (EFSA Scientific Committee, 2018). Regarding manufactured materials, the guidance encourages a first physicochemical characterization to establish whether or not the materials meet the EC definition of NM, and if the material meets the established NM specification, further studies must be performed. Stage 0 of the EFSA guidance consists of investigating the biopersistence rate of NMs to non-nanomaterial under representative gastrointestinal conditions. If a high degradation rate is found, a further nano-specific risk assessment procedure is not necessary. Studies must be done at three different concentration levels and at several gastrointestinal times. The guidance recommends at least two replicates per sample and gastrointestinal time. Particle number concentrations, particle size distribution (PSD), and dissolved metal concentration must be assessed. The EFSA guidance defines NMs as highly degradable if 12% or less of the material (in mass fraction) remains as nanoparticles after completing 30 min of the simulated intestinal digestion (EFSA Scientific Committee, 2018).

PSD and dissolved content can be assessed by single particle–inductively coupled plasma–mass spectrometry (sp-ICP-MS), which is the only currently available technique for simultaneous characterization in size and quantification of NPs with limits of detection below 10 μg L^{-1} (Sadik et al., 2014). Fundamentals of sp-ICP-MS can be found elsewhere (Pace et al., 2011; Laborda et al., 2014; 2016). Metal and metal oxide NPs reach ICP-MS plasma as clouds of metal ions which are detected as pulses at a corresponding mass-to-charge ratio (m/z) in the mass spectrometer. Concentration of NPs in the sample is related to the frequency of detected signal pulses. The metal mass detected in each pulse can be used to estimate particle size by assuming spherical shape and density values (Peters et al., 2015; Mozhayeva & Engelhard, 2020).

The aim of the current work has been the study of the potential biopersistence of TiO_2 and Ag NPs after an *in vitro* gastrointestinal human digestion following EFSA recommendations. The studies were performed with TiO_2 and Ag NPs standards of two different sizes and at three concentration levels each one; the food additive E171, also at three concentration levels; and four seafood (molluscs) and two surimi samples. Changes between gastric and intestinal stages were analysed taking into account NPs concentration, NPs size, and the metal dissolved content after sp-ICP-MS analysis.

2. Experimental

2.1. Instrumentation

A NexION 300X ICP-MS system was used for TiO_2 and Ag NPs characterization and quantification with the Syngistix™ Nano Application software (Perkin Elmer, Shelton, CT, USA). JEM-1010 transmission electron microscope (TEM) from JEOL (Tokyo, Japan) was used for comparative purposes (TEM images). *In vitro* digestion was performed in a Boxcult temperature-controlled incubation chamber (Stuart Scientific, Surrey, UK) with a Rotabit orbital-rocking platform shaker (J.P. Selecta, Barcelona, Spain). Other pieces of equipment were a 50 + DHS pH-meter (XS Instruments, Carpi, Italy), a Raypa UCI–150 ultrasonic cleaner water-bath (17 and 35 kHz, 325 W) from R. Espinar S.L. (Barcelona, Spain), a Laborcentrifugen 2 K15 centrifuge (Sigma, Osterode, Germany), a heating bath from J.P. Selecta, and a domestic Taurus blade grinder (Barcelona, Spain).

2.2. Reagents and materials

Ultrapure water was from a Milli-Q purification device (Millipore Co., Bedford, MA, USA). TiO_2 NPs stock solutions were prepared from TiO_2 nanopowder (99.9% rutile) of 50 and 100 nm (US Research Nanomaterials, Houston, TX, USA). E171 (titanium dioxide) was from Minerals-Water (Rainham, United Kingdom). Ag NPs solutions of 40 and 60 nm with sodium citrate as stabilizer were from Sigma Aldrich (St. Louis, MO, USA). NIST8013 Au NPs (60 nm) certified reference material was from NIST (Gaithersburg, MD, USA). Ionic titanium ($(NH_4)_2TiF_6$ 1000 mg L^{-1}) and ionic silver ($AgNO_3$ 1000 mg L^{-1}) stock standard solutions were from Merck (Darmstadt, Germany). NexION Setup Solution (10 μg L^{-1} Be, Ce, Fe, In, Li, Mg, Pb, and U in 1% nitric acid) was from Perkin Elmer. Pepsin from porcine gastric mucosa, pancreatine from porcine pancreas, and bile salts were from Sigma Aldrich. Hydrochloric acid 37%, nitric acid 65%, and sodium hydrogen carbonate were from Panreac (Barcelona, Spain); 99.5% glycerol was from Merck. Other consumables were Minisart NML hydrophilic non sterile 5.0 μm filters (Sartorius, Goettingen, Germany) and Amicon Ultra-0.5 centrifugal filter units (filters made of regenerated cellulose, 30 kDa nominal molecular weight limit, NMWL) from Merck.

To avoid metal contamination, glassware and plasticware were washed with ultrapure water, kept in 10% (v/v) nitric acid for 48 h, and fully rinsed with ultrapure water before use.

2.3. Bivalve molluscs and crab sticks samples

Biopersistence rate of TiO_2 NPs was studied in mussels (*Mytilus galloprovincialis*), sample denoted as M; and fresh variegated scallops (*Chlamys varia*), denoted as Z24. Ag NPs biopersistence studies were performed with oysters (*Ostrea edulis*), coded as OP; and frozen variegated scallops (coded as Z28). Approximately 1 kg of byssus and shell were removed from each specimen. Soft tissues were washed with ultrapure water and homogenized by mechanical blending.

Surimi (crab stick) samples consisted of a fresh (S6) and a frozen product (S12) which were also homogenized by mechanical blending (approximately 100 g of each sample).

Total Ti and Ag contents, as well as TiO_2 NPs and Ag NPs concentrations in seafood and surimi samples, were previously quantified by ICP-MS and sp-ICP-MS (Taboada-López et al., 2018, 2019a, 2019b).

2.4. In vitro gastrointestinal digestion procedure

The applied simulated *in vitro* digestion was based on previous protocols for iodine in foods (Domínguez-González et al., 2017). Regarding standards and E171 food additive, several volumes of TiO_2 NPs (50 and 100 nm) standards, Ag NPs (40 and 60 nm) standards, and food additive E171 suspensions were added into Erlenmeyer flasks, and ultrapure water was then added up to 50 mL (tested concentrations listed in Table 1). When working with foodstuff, a mass of 5.0 g (wet weight) of molluscs/crab sticks were directly mixed with 50 mL of ultrapure water. For all cases, the pH was adjusted to 2.0 by adding 0.6 M HCl dropwise. Several volumes of gastric solution (0.16 g mL^{-1} pepsin in 0.1 M HCl) were added to provide a concentration of 7.5 mg of gastric solution per mL. Samples were digested at 37 °C in an chamber under orbital-horizontal shaking (150 rpm) for 2.0 h, and the gastric digestion was then stopped by placing the flasks in an ice-bath. The pH of the mixture was then adjusted to 7.0 with 0.2 M NaOH. Intestinal solution (4 mg

Table 1
TiO_2 and Ag concentrations used in the *in vitro* digestion assays.

	STD 50 nm (g TiO_2 L^{-1})	STD 100 nm (g TiO_2 L^{-1})	E171 (g TiO_2 L^{-1})	STD 40 nm (g Ag L^{-1})	STD 60 nm (g Ag L^{-1})
Level 1	6.00×10^{-6}	6.00×10^{-5}	1.33×10^{-3}	5.40×10^{-6}	1.20×10^{-5}
Level 2	6.00×10^{-5}	6.00×10^{-4}		7.40×10^{-6}	1.60×10^{-5}
Level 3	6.00×10^{-4}	6.00×10^{-3}		9.40×10^{-6}	2.00×10^{-5}

mL^{-1} pancreatine and 25 mg mL^{-1} bile salts prepared in 0.1 M $NaHCO_3$) was added to obtain 25% (v/v) intestinal solution concentration. Samples were again incubated for 2.0 h under the same conditions mentioned above.

Four replicates per sample and two blanks were performed for each *in vitro* digestion set. An extra replicate and an extra blank were also prepared to measure NPs concentrations and PSD after pH adjustment at 2.0 and adding the gastric solution (experiment coded as T0). Aliquots of 5.0 mL were taken at 30, 60 and 120 min of the gastric (G30, G60 and G120) and intestinal (I30, I60 and I120) stages. Enzymatic digests from NPs standards and E171 were directly stored at −20 °C; whereas, enzymatic fractions from seafood and crab sticks were filtered (5.0 μm filters) before freezing at −20 °C. Before sp-ICP-MS analysis, thawed enzymatic digests were heated at 90 °C for 10 min to inactivate the residual enzymes (pepsin and pancreatine) in the enzymatic fractions.

2.5. sp-ICPMS measurements

Sp-ICP-MS conditions (Table S1, Electronic Supplementary Information, ESI) were adjusted daily using a solution prepared from NexION Setup Solution and Ti or Ag standards (10 μg L^{-1} of Ti or Ag, and 1.0 μg L^{-1} of Be, Ce, Fe, In, Li, Mg, Pb, and U). Sample flow rate (0.41–0.45 mL min^{-1}) was assessed by pumping (pump speed set at 4 rpm) ultrapure water for 1.0 min and calculating the flow rate by means of the difference of weights before and after ICP-MS aspiration. Transport efficiency (TE%) values within the 2–5% range were directly assessed by Syngistix™ Nano Application software using a gold nanoparticle suspension (60 nm, 518 ng L^{-1}). Sample flow rate, TE(%) value, and Ti and Ag ionic aqueous calibrations (0 to 10 μg L^{-1}) were used by Syngistix™ Nano Application software for assessing NPs concentration, PSD (NPs mean size), and dissolved concentration using NPs density and mass fraction (Pace et al., 2011; Laborda et al., 2014; 2016).

Enzymatic digests were diluted with 1.0% (v/v) glycerol and were sonicated (water-bath, 37 kHz) for 10 min before analysis. Limits of detection (LOD) and quantification (LOQ) were calculated based on three (LOD) or ten (LOQ) times the standard deviation of eleven measurements of a blank, and the slope of the calibration curve. Calculated LOD and LOQ values for TiO_2 NPs concentration were 1.27×10^4 and 4.24×10^4 NPs mL^{-1}, respectively. Regarding Ag NPs, LOD was 1.89×10^3 NPs mL^{-1} and LOQ was 9.22×10^3 NPs mL^{-1}. LOD values for dissolved (ionic) Ti and Ag were 0.295 μg Ti L^{-1} and 0.678 ng Ag L^{-1}; whereas the LOQs were 0.982 μg Ti L^{-1} and 2.26 ng Ag L^{-1}. Finally, LOD size, based on the 3σ/5σ criteria (Lee et al., 2014), were 29.1 nm for TiO_2 NPs and 10.1 nm for Ag NPs (3σ), or 34.5 nm for TiO_2 NPs and 12.0 nm for Ag NPs (5σ).

2.6. TEM-EDX analysis of gastric and intestinal fractions

Gastric and intestinal fractions were filtered through 5.0 μm syringe filters, and then were subjected to cleaning/pre-concentration stage before TEM analysis. The procedure for gastric digests consists of diluting 0.5 mL of the gastric digest with ultrapure water (1:20) and subjecting 0.5 mL aliquots to filtration-ultracentrifugation (30 kDa NMWL) at 14000 g and 4 °C for 20 min (9 ultracentrifugation cycles), and finally at 14000 g and 4 °C for 10 min. Regarding intestinal solutions, 0.5 mL of the sample was subjected to filtration-ultracentrifugation (30 kDa NMWL) at 14000 g and 4 °C for 20 min, and cleaned with 0.5 mL of ultrapure water by ultracentrifugation at 14000 g and 4 °C for 20 min (19 times) and, finally, at 14000 g and 4 °C for 10 min (once). The concentrate in the filter was recovered by placing the filter upside down in a clean microcentrifuge tube and centrifuging at 1000*g* and 4 °C for 2 min. Clean enzymatic extracts (10 μL) were dropped onto a copper grid, wicking on filter paper and air-drying at room temperature before TEM-EDX analysis.

2.7. Statistical analysis

Statgraphics Centurion 18 v18.1.12 (Manugistics Inc., Rockville, MD, USA) software was used for statistical analysis. The Cochran test (95% confidence level) was performed for standard deviation comparison for NPs concentrations and mean sizes (p-values lower than 0.05 imply a statistically significant difference amongst standard deviations, and if p-values are higher than 0.05, standard deviation are not significant different). In both scenarios, a Multiple Range Test was then applied for mean values comparison (detection of homogeneous groups with comparable values of concentrations or sizes).

3. Results and discussion

3.1. TiO_2 NPs biopersistence rate in TiO_2 NPs standards

As shown in Fig. 1 and Table S2 and S3 (electronic supplementary section, ESI), TiO_2 NPs concentration changes were found during the simulated gastric stage ($p < 0.05$). TiO_2 NPs concentrations at 30, 60 and 120 min (G30, G60, and G120 solutions) remain constant and similar to the TiO_2 NPs concentration found at zero time (T0) for 50 and 100 nm TiO_2 NPs standards at the intermediate and high concentrations (Table 1). However, gastric digests from the lowest TiO_2 NPs concentration standards (low concentration level for both 50 and 100 nm TiO_2 NPs, Table 1) showed small differences amongst TiO_2 NPs concentrations at zero time (T0) and after performing the simulated gastric digestion at the selected times. These findings could be attributed to the low concentration of these standards, which could be close to the LOQ of the method. Regarding PSDs, the most frequent sizes, instead of the mean sizes, were used for comparison due to the spread range of size and the high degree of agglomeration of the TiO_2 NPs standards used in this study (characterization confirmed by TEM as shown in Fig. S1, ESI). The most frequent size at the selected gastric digestion times were found to be similar and close to the most frequent size of the solution at T0 ($p < 0.05$). TiO_2 NPs aggregation is expected in the studied solutions since the presence of enzymes and electrolytes that could affect the stability of TiO_2 NPs (aggregation) (Utembe et al., 2015); whereas, TiO_2 NPs dissolution (ionization) during the gastric step was not significant.

Important differences have been observed during the simulated intestinal digestion stage [Fig. 1, and Tables S2 and S3 (ESI)], and TiO_2 NPs concentrations were found to be increased during this stage for all experiments when comparing to TiO_2 NPs concentration in the simulated gastric step. Intestinal conditions must promote TiO_2 ionization and/or TiO_2 NPs dispersion. The higher ionic Ti contents in the simulated intestinal digests compared to those found in simulated gastric digests [Fig. 1, and Tables S2 and S3 (ESI)] suggest that TiO_2 NPs are partially ionized during the intestinal stage. However, this result does not always agree with TiO_2 NPs PSDs because the most frequent sizes in the intestinal digests are not always smaller than those found in the gastric ones. These findings agree with those previously reported for *in vitro* bioaccessibility studies of TiO_2 NPs (Zhong et al., 2017) and other engineered oxide-based nanomaterials such as Fe_3O_4 NPs, CuO NPs, CeO_2 NPs, ZnO NPs (Zhong et al., 2017), and SiO_2 NPs (Peters et al., 2012), in which DLS and SEM analysis support NPs aggregation during the gastric step and NPs dispersion under intestinal conditions. The pH of the digestive solutions has been suggested to be an important parameter. Separated (dispersed) individual nanoparticles are found when the pH is increased from acid (gastric digestion) to neutral (intestinal digestion) (Peters et al., 2012). As reported for SiO_2 NPs (Peters et al., 2012), EDX analysis showed the presence of chloride in the SiO_2 agglomerates, which is expected because hydrochloric acid is a component of the gastric juices. TEM-EDX analysis of the gastric fractions from 50 nm TiO_2 NPs standard at the highest concentration level (Fig. 2) shows highly agglomerated TiO_2 NPs (500 nm) embedded in a diffuse matrix, and EDX microanalysis confirms the presence of chloride in the aggregates (chloride bridges among TiO_2 NPs as previously

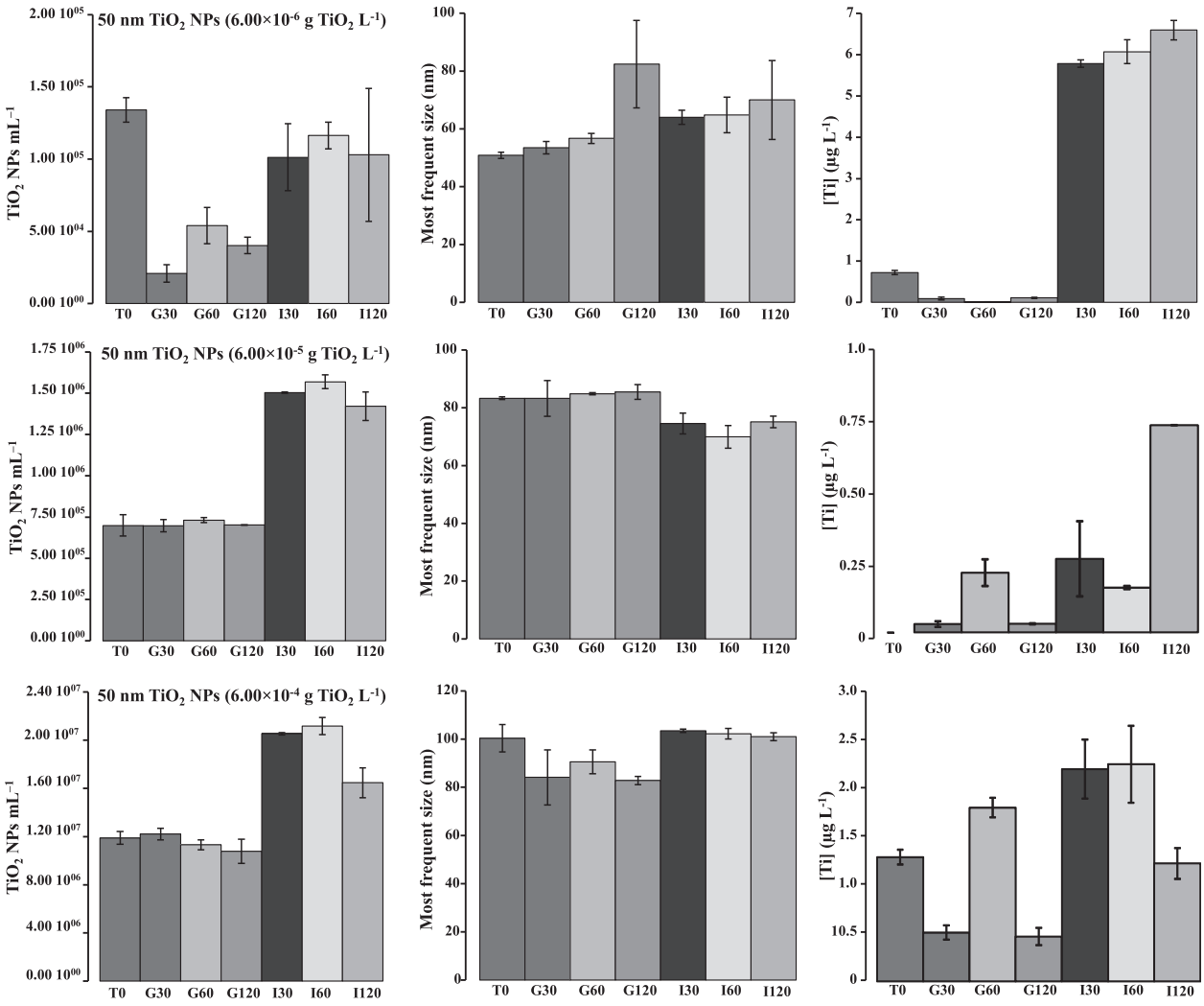

Fig. 1. TiO_2 NPs concentrations, most frequent sizes, and dissolved titanium concentrations at several stages of an *in vitro* gastrointestinal digestion of 50 nm TiO_2 NPs standard at three concentration levels: A) 6.00×10^{-6} g TiO_2 L^{-1}, B) 6.00×10^{-5} g TiO_2 L^{-1}, and C) 6.00×10^{-4} g TiO_2 L^{-1}.

reported for SiO_2 NPs (Peters et al., 2012). On the contrary, chloride was not detected by EDX microanalysis in the intestinal fractions (Fig. 2), and small aggregates and disperse NPs containing Ti were found.

In accordance to EFSA (EFSA Scientific Committee, 2018), the biopersistence rate was calculated as the mass fraction taking into account the TiO_2 NPs concentration before the *in vitro* digestion (T0) and after 30 min of the intestinal stage (I30). The mass of an individual TiO_2 NP was calculated by assuming spherical shape and using the mean size of the PSD, and the TiO_2 density. The mass concentration was then obtained by multiplying the mass of one TiO_2 NP by the TiO_2 NPs concentration. Calculated rates were higher than 100% for 50 nm TiO_2 NPs at the three concentration levels, and higher than 80% for 100 nm TiO_2 NPs, also at the three concentration levels. Biopersistence rates higher than 100% are explained taking into account that TiO_2 NPs dispersion is promoted during the intestinal stage, which implies higher TiO_2 NPs concentrations of lower PSD when comparing with gastric extracts (TiO_2 NPs agglomeration). Agglomeration/dispersion of TiO_2 NPs could lead to a misleading deduction of the biopersistence rate because TiO_2 NPs dispersion during the intestinal stage (I30 extract) leads to a higher TiO_2 NPs concentration than that measured in extracts from the gastric stage and at initial conditions (T0).

The assessed biopersistence rates are higher than the stipulated limit by EFSA (12%) (EFSA Scientific Committee, 2018) and implies that TiO_2 NPs (50 and 100 nm) are unaltered and poorly degradable under gastrointestinal digestion conditions. These findings agree with those reported for solubility (*in vitro* bioaccessibility experiments) of nano-sized metal oxides, TiO_2 NPs included, which showed a very low bioaccessibility of TiO_2 NPs and low toxic effects from the released metal ions (Zhong et al., 2017).

3.2. *TiO_2 NPs biopersistence rate in food additive E171*

Regarding E171 (TEM image in Fig. S2), experiments were performed with higher concentrations than those used for TiO_2 standards (Table 1) since the large PSDs in E171 (lower number of TiO_2 nanoparticles/microparticles in E171 for similar TiO_2 concentrations in TiO_2 NPs standards of low PSD). Similar results to those obtained for 50/100 nm TiO_2 NPs standards have been obtained for E171 experiments (Table S4, ESI), where TiO_2 particles (NPs and mainly microparticles) concentrations were found to be slightly lower after gastric digestion (G30, G60 and G120) than at T0, and no statistically significant differences ($p < 0.05$) were found in the TiO_2 particles concentrations during the gastric digestion process. Similarly, there were no statistically significant differences ($p < 0.05$) for mean sizes and ionic Ti contents during the simulated gastric digestion. Regarding the intestinal digestion stage, higher TiO_2 particles concentrations than those found in gastric digests were measured, results which are in good agreement with those observed for 50/100 nm TiO_2 NPs standards and literature on *in vitro* bioaccessibility (Peters et al., 2012; Zhong et al., 2017). In addition, no statistically significant differences ($p < 0.05$) were found on the TiO_2

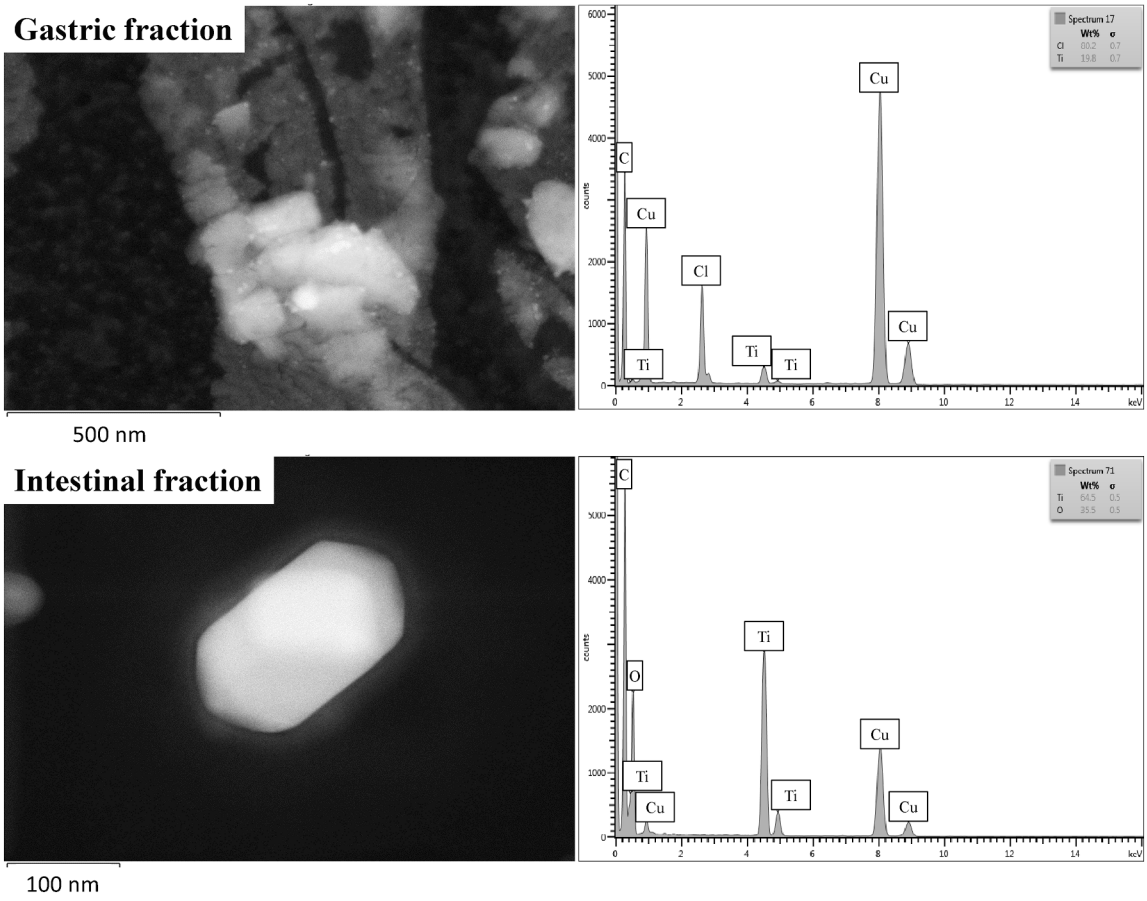

Fig. 2. TEM images and EDX spectra of gastric and intestinal fractions from 50 nm TiO_2 NPs standard at 6.00×10^{-4} g TiO_2 L^{-1}.

particles concentrations, TiO_2 PSD, and dissolved Ti during the intestinal digestion process.

Regarding the biopersistence rate, TiO_2 NPs and TiO_2 microparticles in E171 do not seem to be degradable under gastrointestinal conditions. In accordance with results from 50/100 nm TiO_2 NPs standards, biopersistence rate of TiO_2 NPs and TiO_2 microparticles in E171 was higher than 100%. However, as stated for 50/100 nm TiO_2 NPs standards, agglomeration/dispersion phenomena, mainly because of the presence of organic matter (enzyme residues) in the digests, could misrepresent the biopersistence ratio.

3.3. Ag NPs biopersistence rate in Ag NPs standards

TEM images for the Ag NPs standards used in the experiment are given as ESI (Figure S3). Tables S5 and S6 (ESI) show Ag NPs concentrations, PSD data, and ionic Ag concentrations in gastric and intestinal digests when 40 and 60 nm Ag NPs standards are subjected to the *in vitro* digestion process. Gastric conditions induce a slight increase on Ag NPs concentration at the beginning of the process (G30 experiments for 40 nm and 60 nm Ag NPs at the low and intermediate concentrations), which is more important for 40 nm Ag NPs. Afterward, Ag NPs concentrations are gradually decreased (G60 and G120), except for the experiment with 40 nm Ag NPs at the highest concentration (Fig. S4, ESI). The decrease of Ag NPs concentrations matches, in some cases, with the decrease on the mean sizes (G60 and G120 for 40 nm Ag NPs at the low and intermediate concentrations, and for 60 nm Ag NPs at the highest concentration). On other occasions (60 nm Ag NPs standards at low and intermediate concentration), mean sizes remain constant. Similarly, an increase on the ionic Ag in the gastric digests was observed in some experiments which could imply Ag NPs degradation. These findings agree with those reported by Bove et al. for TEM and DLS analysis of simulated gastric and intestinal digests (dynamic mode) from NM300k Ag NPs (Bove et al., 2017), which have also revealed a high degree of Ag NPs dissolution during the gastric digestion and the simultaneous presence of smaller Ag NPs and large Ag NPs agglomerates (attributed to the organic matrix). sp-ICP-MS, DLS and SEM-EDX also showed Ag NPs agglomeration during the gastric stage in the presence of proteins (pepsin) for experiments with 60 nm Ag NPs, and revealed that reduction in number of particles was caused by their clustering (clusters composed of Ag NPs and chlorine) (Walczak et al., 2012).

Regarding the intestinal stage, an important increase on the Ag NPs concentrations was observed for experiments with the largest size (60 nm NPs, Table S6); whereas, a clear trend was not observed for 40 nm Ag NPs standards (Table S5). PSD was found to be unchanged (gastric and intestinal digests), although ionic Ag concentrations were found to be increased in intestinal digest from 40 nm Ag NPs. In general, these results agree with results by Walczak et al., who also found that the number of Ag NPs rise back to original values after the intestinal digestion (Walczak et al., 2012).

Agglomeration/dispersion phenomena play an important role in an accurate characterization of NPs in complex mediums. However, Ag NPs appear to be more degradable than TiO_2 NPs under gastrointestinal conditions, and biopersistence rates lower than 60% (22, 58, and 31% for 40 nm Ag NPs at low, intermediate and high concentrations, respectively) were calculated according to the EFSA protocol (EFSA Scientific Committee, 2018). However, biopersistence rates were higher than 100% for 60 nm Ag NPs, which could mean that 60 nm Ag NPs are more stable than 40 nm Ag NPs under gastrointestinal conditions and NPs degradability could be dependent on the NPs size.

3.4. TiO_2 NPs biopersistence rate in mollusc and surimi samples

The degradability of TiO_2 NPs 'naturally' present in a mussel sample and in a variegated scallop sample, and TiO_2 NPs used as a food additive in two surimi samples has been studied in accordance with the EFSA guidance. Results (TiO_2 NPs and dissolved Ti concentrations) and mean sizes are listed in Tables S7 and S8 (ESI) and plotted in Figs. 3 and 4. Stability/degradability of TiO_2 NPs appears to be highly dependent of the sample matrix. TiO_2 NPs releasing from surimi during the simulated gastric stage appears to be inefficient and/or TiO_2 NPs and TiO_2 microparticles from E171 contained in surimi are highly clustered under gastric conditions (Fig. 3). High TiO_2 NPs concentrations were measured in enzymatic digests from the intestinal stage (Fig. 3), which is also in good agreement with results from literature (Zhong et al., 2017) and *in vitro* digestion simulations of E171 and 50/100 nm TiO_2 NPs standards.

Variable TiO_2 NPs concentrations were measured in gastric digests when studying fresh mussel and variegated scallop (Fig. 4), and a clear increase on TiO_2 NPs concentrations in the intestinal digests was only observed from variegated scallop (TiO_2 NPs concentration in the intestinal digests from mussel were lower than TiO_2 NPs concentrations in gastric digests and the initial mixture (T0), Fig. 4). Mean sizes of the released TiO_2 NPs and the ionic Ti concentrations in mollusc samples are quite similar during the gastric and the intestinal digestion, which suggests that the *in vitro* process does not degrade the released TiO_2 NPs (Fig. 4). Similarly to TiO_2 NPs standards, TEM-EDX analysis reveals the presence of chloride in the agglomerate TiO_2 NPs from gastric digests from a variegated scallop sample; whereas, dispersed NPs are observed in the intestinal extracts (Fig. 5). However, there is a little increase of the mean sizes of TiO_2 NPs in the intestinal digests when compared to those found in the gastric digests from surimi samples. In addition, the ionic Ti contents in the intestinal digests from surimi are also higher than those measured in the gastric digests.

These findings suggest that the type of NP and the sample matrix contribute to the NPs agglomeration/dispersion phenomena under the same environmental conditions (pH, ionic strength). Therefore, results (trends) from surimi samples are quite similar to those found for experiments with 50 and 100 nm TiO_2 NPs standards, but results are different for fresh molluscs in which TiO_2 NPs are 'naturally' present. These results are important because the reported literature has dealt only with the bioaccessibility of NPs from standards, but the contribution of the food matrix on the overall digestibility process must be taken into account.

Calculated biopersistence rates based on the EFSA guidance (EFSA Scientific Committee, 2018) were higher than 100% in all cases, mainly in surimi samples. This misleading result is attributed to the very low, or even negligible, extracted TiO_2 NPs from molluscs and surimi at initial conditions (T0) (Figs. 3 and 4). Therefore, a biopersistence rate based on concentrations at initial conditions of the gastrointestinal process could be adequate for NPs standards but the criteria cannot be applied to samples (NPs are still linked to the sample matrix at initial conditions).

A biopersistence rate, in which the Ti mass (TiO_2 NPs concentrations) at initial gastrointestinal conditions is changed by the total TiO_2 NPs concentration in the samples (Taboada-López et al., 2018, 2019b), was calculated. Values of 2 and 20% were obtained for mussels and variegated scallops, respectively. However, the biopersistence ratios for surimi samples were higher than 100%, even when using this criterion. This finding is attributed to high TiO_2 (nano)particle dispersion under intestinal conditions resulting in misleading results, mainly due to the large sizes of the particles (Taboada-López et al., 2019b). In conclusion, TiO_2 NPs contained in food (molluscs and surimi) do not seem be degradable.

3.5. Ag NPs biopersistence rate in mollusc samples

Results from oyster (OP) and frozen variegated scallop (Z28) samples are summarized in Table S9 (ESI) and plotted in Fig. S4 (ESI) Ag NPs 'naturally' present in the samples have shown a different behaviour than Ag NPs standards, which implies that sample matrix influence on the bioaccessibility is very important. In addition, Ag NPs (concentration and size) changes along the *in vitro* process were found to be similar in both seafood samples (Fig. S4, ESI). Ag NPs concentration in oyster and variegated scallop samples was lower in the gastric digests (G30, G60, and mainly G120) than at the beginning of the experiment (T0), findings that are not correlated to Ag NPs PSD changes because the Ag NPs mean sizes were found to decrease in the gastric digests. This behaviour is similar to that found in Ag NPs standards (Bove et al., 2017; Walczak et al., 2012) and agrees with the simultaneous presence of smaller Ag NPs and large Ag NPs agglomerates reported for Ag NPs standards in *in*

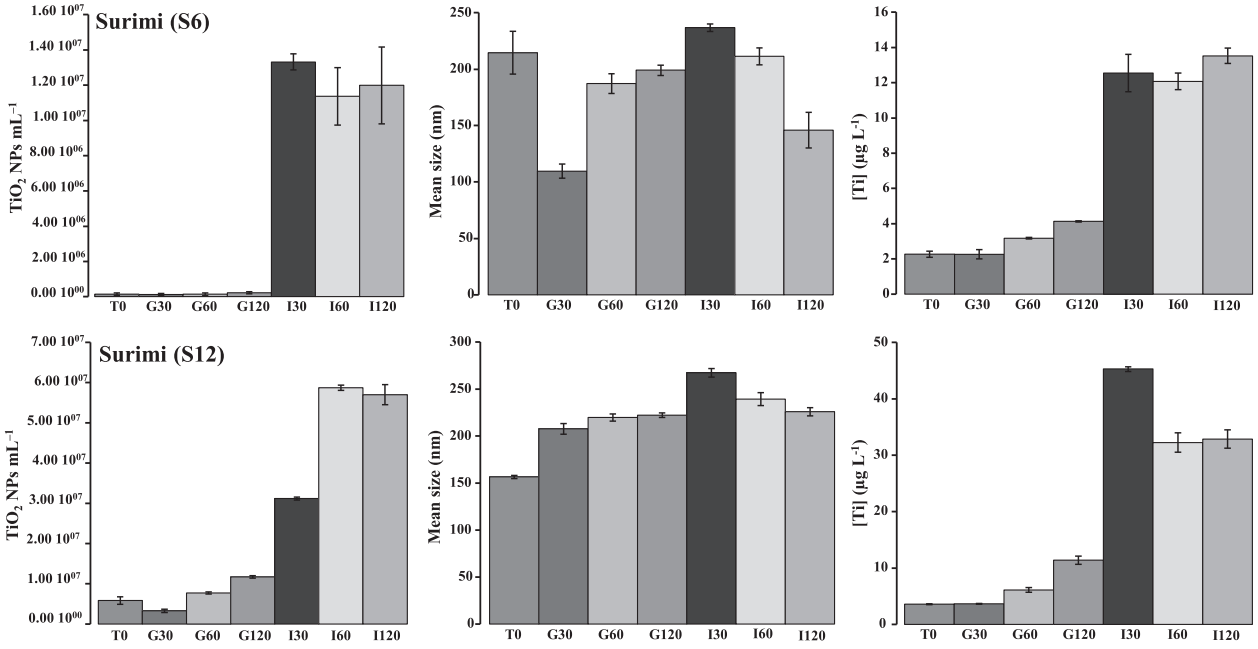

Fig. 3. TiO_2 NPs concentrations, mean sizes, and dissolved titanium concentrations at several stages of an *in vitro* gastrointestinal digestion of surimi (S6 and S12) samples.

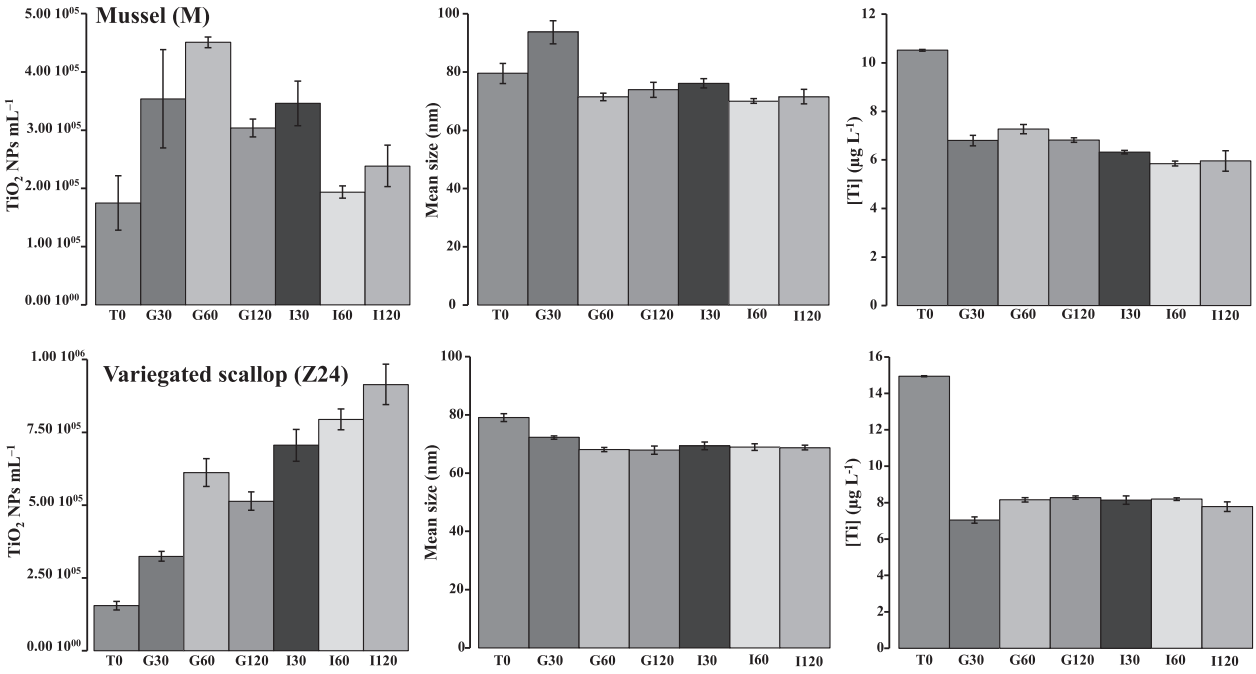

Fig. 4. TiO_2 NPs concentrations, mean sizes, and dissolved titanium concentrations at several stages of an *in vitro* gastrointestinal digestion of mussel (M) and fresh variegated scallop (Z24) samples.

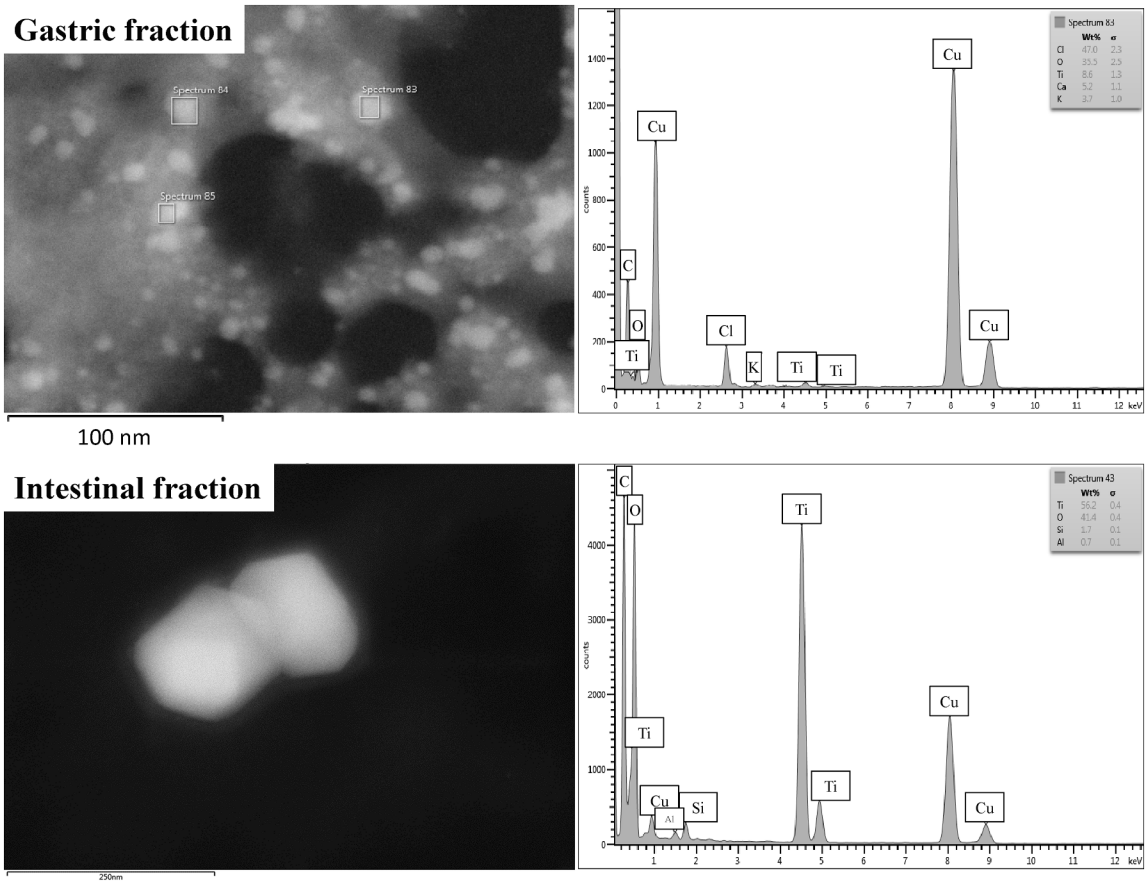

Fig. 5. TEM images and EDX spectra of gastric and intestinal fractions from variegated scallop Z24.

vitro studies (Bove et al., 2017).

An increase on the Ag NPs concentrations in the intestinal digests was observed for both samples, which implies Ag NPs dispersion under the intestinal conditions (Walczak et al., 2012). Ag NPs mean sizes remained constant along the intestinal stage and similar to those measured in the gastric digests for oyster samples, but a significant

increase on mean sizes was found in intestinal digests from variegated scallops. Mean size trends were similar to ionic Ag content, which remained constant during the gastrointestinal process for oysters and was found to be higher in intestinal digests than in gastric digests from variegated scallops. In addition to agglomeration/dispersion as a consequence of the presence of macromolecules (enzymes and degradation products from sample matrix), other factors such as the high trend of Ag NPs to ionization could explain Ag NPs mean size and ionic Ag concentration changes during the *in vitro* gastrointestinal process.

Biopersistence rates were found to be different in both samples (20% in oysters, and higher than 100% in variegated scallops) when using the EFSA criterion. However, biopersistence ratios based on Ag NPs concentrations in the samples (Taboada-López et al., 2019a) instead of Ag NPs at initial conditions (T0) have led to biopersistence values of 2 and 9% for oysters and variegated scallops, respectively, which shows a moderate influence of the sample matrix on the *in vitro* gastrointestinal digestion. The biopersistence values lower than 12% (EFSA Scientific Committee, 2018) suggest that Ag NPs are degraded (ionized) during the gastrointestinal process. However, Ag NPs are highly persistent when applying the EFSA criterion (biopersistence rate based on NPs concentration at initial gastrointestinal conditions).

4. Conclusions

In general, nanoparticle agglomeration during *in vitro* gastric digestion and nanoparticle dispersion under intestinal conditions has been observed when subjecting TiO_2 NPs and Ag NPs standards of different PSDs. However, studied Ag NPs standards have shown a high size-dependent behaviour because 40 nm Ag NPs agglomeration was observed at the early stages of gastric digestion; whereas, ionization phenomena appears to dominate during the gastric digestion stage for experiments with 60 nm Ag NPs standards. In addition, sample matrix constituents have been found to influence TiO_2 NPs and Ag NPs bioaccessibility, while TiO_2 NPs 'naturally' present in bivalve molluscs showed slow NPs release along the *in vitro* gastrointestinal digestion; whereas, TiO_2 NPs behaviour from surimi samples was quite similar to that found when studying TiO_2 particles (NPs plus microparticles) from E171. Regarding Ag NPs in molluscs, different trends were observed depending on the sample, and both agglomeration/dispersion and Ag NPs ionization phenomena have been found to be important.

Biopersistence rates were higher than 100% in TiO_2 NPs standards and TiO_2 NPs/ TiO_2 microparticles from E171, which shows that these nano/microparticles are not degraded under simulated gastrointestinal conditions. However, Ag NPs have been found to be more degradable than TiO_2 NPs, and the biopersistence rate was dependent on the Ag NPs size. A higher digestibility of Ag NPs (lower biopersistence rate) was also found in seafood samples than that found for TiO_2 NPs in molluscs and surimi, but biopersistence rates were higher than the limit set by the EFSA (12%). Biopersistence rate in accordance with the EFSA guidance (EFSA Scientific Committee, 2018) was defined for studying the effect of NPs suspensions (standards and NM-based food additives). However, the application of the defined biopersistence rate to food samples is not straightforward because the NPs concentrations at the beginning of the experiment (T0 experiments) are going to be very low (NPs are linked to sample matrix components and are not going to be assessed because they have not yet been released). A biopersistence rate based on the initial NPs concentrations at T0 could thus lead to rates higher than 100% (misleading results). We therefore suggest changing the NPs concentrations at initial gastrointestinal conditions for total NPs concentration in the sample to improve the assessment of the biopersistence rate when applying the EFSA guidance to food samples. Finally, *in vitro* experiments by fortifying seafood products with TiO_2 and Ag NPs standards, and also with E171, would be welcome for a better elucidation of the effect of the sample matrix on the biopersistence rate of TiO_2 and Ag NPs (and also TiO_2 particles).

CRediT authorship contribution statement

María Vanesa Taboada-López: Formal analysis, Investigation, Validation, Visualization, Writing - original draft. **Gemma Vázquez-Expósito:** Formal analysis, Investigation, Validation. **Raquel Domínguez-González:** Supervision, Validation, Writing - review & editing. **Paloma Herbello-Hermelo:** Data curation, Supervision, Validation. **Pilar Bermejo-Barrera:** Resources, Project administration, Funding acquisition, Writing - review & editing. **Antonio Moreda-Piñeiro:** Software, Validation, Writing - review & editing, Supervision.

Declaration of Competing Interest

The authors declare that they have no known competing financial interests or personal relationships that could have appeared to influence the work reported in this paper.

Acknowledgements

The authors wish to acknowledge the financial support of the Ministerio de Economía y Competitividad (project INNOVANANO, reference RT2018-099222-B-100), the European Union (Interreg POCTEP, project ACUINANO, reference 07-12-ACUINANO_1_E), and the *Xunta de Galicia* (*Grupo de Referencia Competitiva*, grant number ED431C2018/19; and Program for Development of a Strategic Grouping in Materials – AEMAT, grant number ED431E2018/08). The authors are also grateful to Dr. Enrique Carbo and Dr. Laura Rodríguez-Lorenzo from the International Iberian Nanotechnology Laboratory (Braga, Portugal) for TEM assistance. M.V. Taboada-López would like to thank the *Xunta de Galicia* and the European Social Fund (FSE) for a pre-doctoral grant.

Appendix A. Supplementary data

Supplementary data to this article can be found online at https://doi.org/10.1016/j.foodchem.2021.130002.

References

Akter, M., Sikder, M. T., Rahman, M. M., Ullah, A. K. M. A., Hossain, K. F. B., Banik, S., … Kurasaki, M. (2018). A systematic review on silver nanoparticles-induced cytotoxicity: Physicochemical properties and perspectives. *Journal of Advanced Research, 9*, 1–16.

Bove, P., Malvindi, M. A., Kote, S. S., Bertorelli, R., Summa, M., & Sabella, S. (2017). Dissolution test for risk assessment of nanoparticles: A pilot study. *Nanoscale, 9*, 6315–6326.

Consumer Products Inventory. An inventory of nanotechnology-based consumer products introduced on the market, http://www.nanotechproject.org/cpi (accessed on January 7th 2020).

Domínguez-González, M. R., Chiocchetti, G. M., Herbello-Hermelo, P., Vélez, D., Devesa, V., & Bermejo-Barrera, P. (2017). Evaluation of iodine bioavailability in seaweed using *in vitro* methods. *Journal of Agricultural and Food Chemistry, 65*, 8435–8442.

dos Santos, C. A., Ingle, A. P., & Rai, M. (2020). The emerging role of metallic nanoparticles in food. *Applied Microbiology and Biotechnology, 104*, 2373–2383.

EFSA Scientific Committee. (2018). Guidance on risk assessment of the application of nanoscience and nanotechnologies in the food and feed chain: Part 1, human and animal health. *EFSA Journal, 16*, 5327–5395.

Geiss, O., Ponti, J., Senaldi, C., Bianchi, I., Mehn, D., Barrero, J., … Anklan, E. (2020). Characterisation of food grade titania with respect to nanoparticle content in pristine additives and in their related food products. *Food Additives and Contaminants A, 37*, 236–253.

Holland, L., & Zhong, W. (2018). Analytical developments in advancing safety in nanotechnology. *Analytical and Bioanalytical Chemistry, 410*, 6037–6039.

Laborda, F., Bolea, E., & Jiménez-Lamana, J. (2014). Single particle inductively coupled plasma mass spectrometry: A powerful tool for nanoanalysis. *Analytical Chemistry, 86*, 2270–2278.

Laborda, F., Bolea, E., & Jiménez-Lamana, J. (2016). Single particle inductively coupled plasma mass spectrometry for the analysis of inorganic engineered nanoparticles in environmental samples. *Trends in Environmental Analytical Chemistry, 9*, 15–23.

Laloux, L., Polet, M., & Schneider, Y. J. (2017). Interaction between ingested-engineered nanomaterials and the gastrointestinal tract: In vitro toxicology aspects. In M. A. V. Axelos, & M. Van-de-Voorde (Eds.), *Nanotechnology in agriculture and food science* (pp. 311–331). Weinheim: Wiley-VCH Verlag GmbH & Co.

Lee, S., Bi, X., Reed, R. B., Ranville, J. F., Herckes, P., & Westerhoff, P. (2014). Nanoparticle size detection limits by single particle ICP-MS for 40 elements. *Environmental Science and Technology, 48*, 10291–10300.

Le-Guével, X. (2017). Overview of inorganic nanoparticles for food science applications. In M. A. V. Axelos, & M. Van-de-Voorde (Eds.), *Nanotechnology in agriculture and food science* (pp. 197–207). Weinheim: Wiley-VCH Verlag GmbH & Co.

McClements, D. J., Xiao, H., & Demokritou, P. (2017). Physicochemical and colloidal aspects of food matrix effects on gastrointestinal fate of ingested inorganic nanoparticles. *Advances in Colloid and Interface Science, 246*, 165–180.

Mei, L., & Wang, Q. (2020). Advances in using nanotechnology structuring approaches for improving food packaging. *Annual Review of Food Science and Technology, 11*, 339–364.

Mozhayeva, D., & Engelhard, C. (2020). A critical review of single particle inductively coupled plasma mass spectrometry – A step towards an ideal method for nanomaterial characterization. *Journal of Analytical Atomic Spectrometry, 35*, 1740–1783.

Murugan, K., Choonara, Y. E., Kumar, P., Bijukumar, D., du Toit, L. C., & Pillay, V. (2015). Parameters and characteristics governing cellular internalization and trans-barrier trafficking of nanostructures. *International Journal of Nanomedicine, 10*, 2191–2206.

Ogunsona, E. O., Muthuraj, R., Ojogbo, E., Valerio, O., & Mekonnen, T. H. (2020). Engineered nanomaterials for antimicrobial applications: A review. *Applied Materials Today, 18*, Article 100473.

Pace, H. E., Rogers, N. J., Jarolimek, C., Coleman, V. A., Higgins, C. P., & Ranvill, J. F. (2011). Determining transport efficiency for the purpose of counting and sizing nanoparticles via single particle inductively coupled plasma mass spectrometry. *Analytical Chemistry, 83*, 9361–9369.

Peters, R., Kramer, E., Oomen, A. G., Herrera Rivera, Z. E., Oegema, G., Tromp, P. C., … Bouwmeester, H. (2012). Presence of nano-sized silica during in vitro digestion of foods containing silica as a food additive. *ACS Nano, 6*, 2441–2451.

Peters, R., Herrera-Rivera, Z., Undas, A., van der Lee, M., Marvin, H., Bouwmeester, H., & Weigel, S. (2015). Single particle ICP-MS combined with a data evaluation tool as a routine technique for the analysis of nanoparticles in complex matrices. *Journal of Analytical Atomic Spectrometry, 30*, 1274–1285.

Sadik, O. A., Du, N., Kariuki, V., Okello, V., & Bushlyar, V. (2014). Current and emerging technologies for the characterization of nanomaterials. *ACS Sustainable Chemistry and Engineering, 2*, 1707–1716.

Sharma, R., Jafari, S. M., & Sharma, S. (2020). Antimicrobial bio-nanocomposites and their potential applications in food packaging. *Food Control, 12*, Article 107086.

Taboada-López, M. V., Iglesias-López, S., Herbello-Hermelo, P., Bermejo-Barrera, P., & Moreda-Piñeiro, A. (2018). Ultrasound assisted enzymatic hydrolysis for isolating titanium dioxide nanoparticles from bivalve mollusk before sp-ICPMS. *Analytica Chimica Acta, 1018*, 16–25.

Taboada-López, M. V., Alonso-Seijo, N., Herbello-Hermelo, P., Bermejo-Barrera, P., & Moreda-Piñeiro, A. (2019). Determination and characterization of silver nanoparticles in bivalve molluscs by ultrasound assisted enzymatic hydrolysis and sp-ICPMS. *Microchemical Journal, 148*, 652–660.

Taboada-López, M. V., Herbello-Hermelo, P., Domínguez-González, R., Bermejo-Barrera, P., & Moreda-Piñeiro, A. (2019). Enzymatic hydrolysis as a sample pre-treatment for titanium dioxide nanoparticles assessment in surimi (crab sticks) by single particle ICP-MS. *Talanta, 195*, 23–32.

The European Commission. Commission, Recommendation (UE) 2011/696 of 18 October 2011 on the definition of nanomaterial, Official Journal of the European Union L 275, 58 (2011) 38–40.

Utembe, W., Potgieter, K., Stefaniak, A. B., & Gulumian, M. (2015). Dissolution and biodurability: Important parameters needed for risk assessment of nanomaterials. *Particle and Fibre Toxicology, 12*, 11. https://doi.org/10.1186/s12989-015-0088-2.

Venkatasubbu, G. D., Baskar, R., Anusuya, T., Seshan, C. A., & Chelliah, R. (2016). Toxicity mechanism of titanium dioxide and zinc oxide nanoparticles against food pathogens. *Colloids and Surfaces B, 148*, 600–606.

Walczak, A. P., Fokkink, R., Peters, R., Tromp, P., Herrera Rivera, Z. E., & Rietjens, I. M. C. M. (2012). Behaviour of silver nanoparticles and silver ions in an in vitro human gastrointestinal digestion model. *Nanotoxicology, 7*, 1198–1210.

Weir, A., Westerhoff, P., Fabricius, L., Hristovski, K., & von Goetz, N. (2012). Titanium dioxide nanoparticles in food and personal care products. *Environmental Science and Technology, 46*, 2242–2250.

Yang, Y., Doudrick, K., Bi, X., Hristovski, K., Herckes, P., Westerhoff, P., & Kaegi, R. (2014). Characterization of food-grade titanium dioxide: The presence of nanosized particles. *Environmental Science and Technology, 48*, 6391–6400.

Yemmireddy, V. K., & Hung, Y. C. (2015a). Selection of photocatalytic bactericidal titanium dioxide (TiO_2) nanoparticles for food safety applications. *LWT-Food Science and Technology, 61*, 1–6.

Yemmireddy, V. K., & Hung, Y. C. (2015b). Effect of food processing organic matter on photocatalytic bactericidal activity of titanium dioxide (TiO_2). *International Journal of Food Microbiology, 204*, 75–80.

Zheng, K., Setyawati, M. I., Leong, D. T., & Xie, J. (2018). Antimicrobial silver nanomaterials. *Coordination Chemistry Reviews, 357*, 1–17.

Zhong, L., Yu, Y., Lian, H.-Z., Hu, X., Fu, H., & Chen, Y.-J. (2017). Solubility of nano-sized metal oxides evaluated by using in vitro simulated lung and gastrointestinal fluids: Implication for health risks. *Journal of Nanoparticle Research, 19*, 375.